

## Original Paper

# Improving Bone Regeneration Using Chordin siRNA Delivered by pH-Responsive and Non-Toxic Polyspermine Imidazole-4,5-Imine

Chuangdong Wang<sup>a</sup> Fei Xiao<sup>a</sup> Yaokai Gan<sup>c</sup> Weien Yuan<sup>b</sup> Zhanjing Zhai<sup>c</sup>  
Tuo Jin<sup>b</sup> Xiaodong Chen<sup>a</sup> Xiaoling Zhang<sup>a</sup>

<sup>a</sup>Department of Orthopedic Surgery, Xin Hua Hospital Affiliated to Shanghai Jiao Tong University School of Medicine (SJTUSM), Shanghai, <sup>b</sup>School of Pharmacy, Shanghai Jiao tong University, 800 Dongchuan Road, Shanghai, <sup>c</sup>Shanghai Key Laboratory of Orthopaedic Implant, Department of Orthopaedic Surgery, Shanghai Ninth People's Hospital, Shanghai Jiao Tong University School of Medicine, Shanghai, P. R. of China

## Key Words

Human bone marrow mesenchymal stem cells • Chordin • Bone morphogenetic protein-2 • Polyspermine imidazole-4 • 5-imine • Osteogenesis

## Abstract

**Background/Aims:** Bone nonunion remains a challenge for orthopaedists. The technological advancements that have been made in precisely silencing target genes have provided promising methods to address this challenge. **Methods:** We detected the expression levels of the bone morphogenetic protein (BMP) inhibitors Chordin, Gremlin and Noggin using real-time PCR in bone mesenchymal stem cells (BMSCs) isolated from patients with normal fracture healing and those with bone nonunion. Moreover, we detected the expression of Chordin, Gremlin and Noggin during the osteogenic differentiation of human BMSCs (hBMSCs) using real-time PCR and Western blot. We delivered Chordin siRNA to hBMSCs using a previously reported cationic polymer, polyspermine imidazole-4,5-imine (PSI), as a pH-responsive and non-cytotoxic transfection agent. The apoptosis and cellular uptake efficiency were analysed by flow cytometry. **Results:** We identified Chordin as the most appropriate potential therapeutic target gene for enhancing the osteogenic differentiation of hBMSCs. Chordin knockdown rescued the osteogenic capacity of hBMSCs isolated from patients with bone nonunion. Highly efficient knockdown of Chordin was achieved in hBMSCs using PSI. Chordin knockdown promoted hBMSC osteogenesis and bone regeneration *in vitro* and *in vivo*. **Conclusions:** Our results suggest that Chordin is a potential target for improving osteogenesis and bone nonunion therapy and that responsive and non-toxic cationic polyimines such as PSI are therapeutically feasible carriers for the packaging and delivery of Chordin siRNA to hBMSCs.

© 2018 The Author(s)  
Published by S. Karger AG, Basel

C. Wang and F. Xiao contributed equally to this work.

Xiaoling Zhang

Department of Orthopedic Surgery, Xin Hua Hospital Affiliated to Shanghai Jiao Tong University School of Medicine (SJTUSM), Shanghai (China)  
Tel. +86- 21-54923338, Fax +86-21-54923338, E-Mail xlzhang@shsmu.edu.cn

## Introduction

Bone nonunion is a serious problem that may occur following bone fractures and segmental defects, resulting in a heavy financial burden for both the patient and for the government due to health care costs and the reduced ability of the patient to work [1, 2]. Approximately 5% to 10% of fractures result in bone nonunion. An improved understanding of bone biology could facilitate the treatment of bone nonunion [1]. Upon bone damage, bone mesenchymal stem cells (BMSCs) migrate to the damaged portion of bone and differentiate into osteoblasts, which secrete large amounts of extracellular matrix (ECM) to promote bone fracture healing. The migration and osteogenic differentiation of BMSCs are tightly regulated by various cellular signals [3-8], and *in vitro* and *in vivo* studies have shown that bone morphogenetic proteins (BMPs) play a critical role in osteogenic differentiation and bone formation [9-11]. BMPs combine with type I and II receptors on the cell surface to form a complex and activate the Smad signalling pathways, which regulate osteogenic gene expression [12, 13], suggesting that manipulation of BMP signalling may be employed as a therapeutic approach to treat bone nonunion. However, this technique has several key disadvantages, as these factors must be used at supraphysiological concentrations, are short-lived and expensive, and result in many side effects [14-17].

Recently, the role of BMP inhibitors and the extent to which they can be used as a control mechanism have received much attention [18-20]. The time- and concentration-dependent expression of both BMPs and BMP inhibitors plays a vital role in bone development and bone fracture healing [19]. The expression profiles of BMPs and their inhibitors in human BMSCs (hBMSCs) from patients with normal bone fracture healing and those with bone nonunion are unknown. BMP-mediated osteogenic differentiation is closely regulated by extracellular BMP inhibitors, including Noggin, Chordin and Gremlin [21], suggesting that BMP inhibitors in BMSC are ideal therapeutic targets for bone healing. However, the role of BMP inhibitors in BMSC osteogenesis, bone healing and bone nonunion is not well understood.

Molecular therapeutics (including gene therapy, small interfering RNAs (siRNAs) and small molecular antagonists) might provide a good solution for blocking BMP inhibitors, which could eliminate the need for high doses of BMPs to stimulate bone healing. siRNAs are nucleic acid fragments 21-23 nucleotides long that can specifically suppress the expression of a target gene via their strict design [22]. Thus, siRNA provides a solution for drug design and a new method of developing customizable medicines. Currently, the major challenge in gene therapy is developing a transfection vector that exhibits biocompatibility, multifunctionality, stimulus responsiveness, high loading capacity and high transfection efficiency [23]. Polyethyleneimine (PEI) has long been used for gene delivery because of its high cationic charge density and ability to condense siRNA and escape the endosome [24-28]. PEI25kDa is a classical gene delivery vector that does not consist of biodegradable chemical linkages; hence, PEI25kDa does not meet the requirement for clinical application because of its high cytotoxicity and nonbiodegradability. Spermine is a widespread endogenous multi-amino monomer whose major function in the body is nucleic acid condensation. Many studies have used spermine as a building block to synthesize suitable siRNA carriers [27-29]. Recently, we developed a pH-responsive and non-toxic siRNA carrier system, polyspermine imidazole-4, 5-imine (PSI), which offers an example of a cationic polymer capable of condensing siRNA into a polyplex and releasing the siRNA from the endosome into the cytoplasm [22]. One of the unique characteristics of PSI is that at endosomal pH values, it degrades into spermine with two free amino groups, which is non-toxic to hBMSCs, and a safe metabolite. This safe and efficient synthetic carrier system may allow the revolutionary siRNA technology to be used in bone regeneration therapy.

In the present study, we examined the naturally occurring levels of BMPs and their inhibitors in hBMSCs isolated from patients with bone nonunion and normal fracture healing, evaluated the expression of BMP inhibitors during hBMSC osteogenic differentiation, and identified Chordin as an ideal target for enhancing the osteogenic differentiation of hBMSCs isolated from patients with bone nonunion. We then examined the cytotoxic and apoptotic

effects and transfection efficiency of PSI in hBMSCs and detected the osteogenic activity of hBMSCs transfected with PSI/Chordin-siRNA *in vitro* and *in vivo*. Our results regarding the effect of PSI/Chordin knockdown on the bone regenerative abilities of hBMSCs will facilitate the design of novel MSC-based therapies to treat bone nonunion.

## Materials and Methods

### *Preparation and characterization of PSI/siRNA and PEI25kDa/siRNA polyplexes*

PSI was prepared as described in our report in 2012 [22]. Branched PEIs (25 kDa, 800 Da) were purchased from Sigma-Aldrich (St. Louis, MO, USA). PSI/siRNA and PEI25kDa/siRNA polyplexes were prepared by mixing 100  $\mu$ L of RNase-free water containing different concentrations of PSI or PEI25kDa with 100  $\mu$ L of RNase-free water containing siRNA (2  $\mu$ M) to obtain the desired N/P ratio, followed by gentle mixing for 30 s and incubation at room temperature for 30 min.

### *hBMSC osteogenic differentiation*

hBMSCs were donated by patients who provided written informed consent, and this experiment was approved by the Institutional Ethics Committee of Shanghai Jiao Tong University School of Medicine (SJTUSM). hBMSCs were obtained from two sources. The first source was patients with bone nonunion; the second source was patients with normal fracture healing. For osteogenic differentiation, hBMSCs at passage 3 were seeded at  $1 \times 10^5$  cells/well in a six-well plate and cultured in BM. When confluence was reached, the cells were cultured in BM or OM (BM supplemented with 100 ng/mL BMP-2 (#120-02, Peprotech, USA)). BMP-4 (#120-05), BMP-6 (#120-06), BMP-7 (#120-03) and BMP-9 (#120-7) were purchased from Peprotech. The culture medium was changed every 3 days. Alizarin Red S staining (#A5533, Sigma Aldrich, USA) was performed after 21 days of osteogenic culture. To quantify osteogenic differentiation, 2 mL or 1 mL of 0.1 N NaOH was added to each well of a 6-well or 12-well plate, respectively, to dissolve the extracellular calcium deposits, and then 100  $\mu$ L of the dissolved solution was analysed using a microplate reader (Infinite M200 PRO, TECAN, Switzerland) at 548 nm.

### *Lentiviral transduction overexpression studies*

The human Chordin gene was ligated into the pLVX-IRES-Puro vector using PCR primers to amplify the coding region. The pLVX-IRES-Puro and pLVX-IRES-Puro-Chordin constructs were transfected into the viral packaging cell line HEK293T together with pSPAX2 and pMD2.G. Viral supernatants were used to infect hBMSCs.

### *MTT assay*

To determine whether PSI and PSI and siRNA polyplexes were cytotoxic to hBMSCs, we performed an MTT (#M5655, Sigma, USA) assay as follows. hBMSCs at passage 3 were seeded at  $1 \times 10^4$  cells/well in 96-well plates and cultured for 24 h. The culture medium was subsequently replaced with medium containing different concentrations of PSI or polyplexes at varying N/P ratios. After incubation at 37 °C under 5% CO<sub>2</sub> for 4 h, the culture medium was replaced with 200  $\mu$ L/well MTT reagent (0.5 mg/mL MTT dissolved in complete culture medium), and the plates were incubated for another 4 h at 37 °C under 5% CO<sub>2</sub>. The unreacted MTT reagent was removed, and the formazan crystals were dissolved by adding 200  $\mu$ L of dimethyl sulfoxide (DMSO) to each well. The OD was measured using a microplate reader (Infinite M200 PRO, TECAN, Switzerland) at a wavelength of 570 nm and a reference wavelength of 630 nm. Cell viability was calculated as [(OD570 – OD630) test]/[(OD570 – OD630) control].

### *Real-time PCR*

The total RNA was isolated from hBMSCs using TriPure Isolation Reagent (#93956520, Roche, Switzerland) according to the manufacturer's instructions. RNA samples (1  $\mu$ g) were reverse transcribed using a Prime Script RT Master Mix cDNA Synthesis Kit (#RR036A-1, Takara, Japan) to obtain first-strand cDNA. Real-time PCR was performed on a Light-cycler 480 (Roche, Switzerland) using SYBR Premix ExTaq™ (#RR420a, Takara, Japan) according to the manufacturer's instructions. The real-time PCR conditions were as follows: denaturation at 95 °C for 30 s, followed by 50 cycles of 95 °C for 10 s and 60 °C for 30 s.  $\beta$ -actin

was used as the housekeeping gene. The sequences of the gene primers used are listed in Table 1.

*Chordin knockdown and cellular uptake efficiency*

Chordin, Noggin and Gremlin expression was knocked down using siRNA. The sense and antisense sequences of the Chordin, Noggin and Gremlin siRNAs are listed in Table 2. The siRNA sequences were synthesized by Shanghai GenePharma Co., Ltd. A FITC fluorescein-conjugated negative control siRNA (GenePharma, Shanghai, China) was used to assess the transfection efficiency of PSI. The FITC fluorescein-conjugated negative control siRNA was not homologous to any known gene, thus avoiding nonspecific effects on cellular gene expression caused by the introduction of the oligonucleotide into the cells. hBMSCs were seeded under the same experimental conditions and transfected with the FITC fluorescein-conjugated negative control at varying N/P ratios using different polymers. After incubation for 4 h, the proportion of transfected cells was measured using FACS analysis (Becton Dickinson Biosciences, San Diego, CA) and FlowJo flow cytometry analysis software (Tree Star, USA). The hBMSCs were then transfected with a Cy3-fluorescein-conjugated negative control at optimal N/P ratios using different polymers. After incubation for 1 h, the nuclei and lysosomes of hBMSCs were labelled with Hoechst 3342 (#H3570, Life Technologies, USA) and LysoTracker (#L7526, Life Technologies, USA), respectively, and observed via laser confocal microscopy (Cell Observer, ZEISS, Germany).

*Apoptosis and JC-1 staining*

hBMSCs at passage 3 were seeded onto a six-well plate at a density of  $1 \times 10^5$  cells/well and cultured in complete BM. After 24 h of culture, the complete medium was replaced with 1 mL of Opti-MEM (#31985062, Life Technologies, USA) containing polyplexes with different N/P ratios. After 4 h of incubation, the cells were harvested and washed with cold PBS. The hBMSCs were stained using an apoptosis analysis kit (#V13241, Life Technologies, USA) according to the manufacturer's instructions. The stained cells were immediately analysed by flow cytometry by using the FlowJo flow cytometry analysis software (Tree Star, USA). After transfection with different polyplexes, the cells were stained with a LIVE/DEAD Viability/Cytotoxicity Kit (#L-3224, Life Technologies, USA) and a JC-1 analysis kit (#C2005, Beyotime, China) according to the manufacturer's instructions. The stained hBMSCs were immediately observed by laser confocal microscopy (Cell Observer, ZEISS, Germany).

*Western blot analysis*

For Western blot analysis, hBMSCs were lysed on ice for 30 min in lysis buffer. The protein fractions were collected by centrifugation at 15,000 g for 10 min at 4 °C, subjected to 10% SDS-PAGE, and finally transferred onto nitrocellulose membranes. The transferred membranes were blocked with 5% BSA and then incubated with specific antibodies overnight at 4 °C. A horseradish peroxidase-labelled secondary antibody was added and visualized using an enhanced chemiluminescence detection system (#WBKLS0500,

**Table 1.** List of primers used for real-time PCR analysis

Gene name	Forward primer(5'-3')	Reverse primer(5'-3')
Chordin	TTCGGGGGAAGGCTATG	ACTCTGGTTGATGTTCTTGAG
Cerberus	TCCAGGGACTCAGATAGTGAGC	GCAGGCTCCCAATGTAAGTCA
Gremlin	CGGAGCGCAAATACCTGAAG	GGTTGATGATGTTGGGACTGT
Usag1	AACAGCACGTTGAATCAAGCC	GCCATCAGAGATGTATTTGGTGG
Sclerostin	ACACAGCCTTCCGTTAGTG	GGTTTCATGGCTTGTGTCTCC
Coco	AAGTGATCCAGGGGATGTGA	GATGATTCGGAGGGGATGG
Prdc	ATCCCTCGCCTTACAAGGA	TCTTGACACAGTCACTCTTGA
DAN	CATGTGGGAGATTGTGACGCT	CCTCGTACTAGGCTCTTG
Twisted Gastrulation (Twsg1)	ATTGGAACATCGTTTCTTCCCT	ACCAGCGATATTTGGATGCTC
Crossveinless	TTTATCACAGACAACCTTGCAT	TCCTGGCACTGGCTAGAA
Noggin	CCATGCCGAGCGAGATCAAA	TCGGAATGATGGGGTACTGG
BMP-2	ACCCGCTGTCTTCTAGCGT	TTTCAGGCCGAACATGCTGAG
BMP-4	ATGATTCCTGGTAACCGAATGC	CCCGTCTCAGGTATCAAAC
BMP-7	TCGGCACCCATGTTTCATGC	GAGGAAATGGCTATCTTGAGG
ID1	CTGCTTACGACATGAACGG	GAAGGTCCTGTATGTAGTAG
ID2	AGTCCGTTGAGGTCGTTAG	AGTCCGTTGATGTATAGCAGG
ID3	GAGAGGCACTCAAGCTTAGCC	TCCTTTTGTGTTGGAGTAGAC
ID4	TCCGGCCCAACAAGAAGTC	CCAGGATGTAGTCCATCAAGTG
BMP-6	TGTTGGACACCGTGTAGTAT	AACCCACAGATGCTAGTGGC
BMP-9	CGCACATGTTGGACCGCTG	AGAAAGTGAAGGTGGATTTCC
Sp7 transcription factor (OSX)	CCTCTCGGGACTCAACAAC	AGCCCATTAGTGTGTAAAGG
Osteocacin(OCN)	GAAGCCAGCGGTGCA	CAC TACTCGTGCCTCC
collagen, type I, alpha1(Col1a1)	GAGGGCCAAGACGAAGACATC	CAGTACAGCTATCGCACAAAC
GAPDH	ACAACCTTGGTATCGTGAAGG	GCCATCACGCCACAGTTTC

**Table 2.** The sense and antisense sequences of the Chordin, Noggin and Gremlin siRNA

siRNA name		Sequence (5'-3')
Chordin siRNA	Sense	GGUGCACAUAGCCAACCAATT
	Antisense	UUGGUUGGCUAUGUGACCTG
noggin siRNA	Sense	GCUGGAUUCUCAUCCAGUATT
	Antisense	UACUGGAUGGAAUCCAGCCG
Gremlin siRNA	Sense	AGAAUCUGGUUGUUUAGGUC
	Antisense	CCUAAAACAACCAGAUUCUUA

Millipore, MA) according to the manufacturer's instructions. The primary antibodies used are as follows: Chordin goat pAb (1:500, #sc-23557, Santa Cruz, USA), Runx2 mouse mAb (1:1000, #ab76956, Abcam, USA), phospho-SMAD/5/8 rabbit pAb (1:1000, #4086, Cell Signaling Technology, USA), SMAD1 rabbit mAb (1:1000, #6944, Cell Signaling Technology, USA), and GAPDH rabbit mAb (1:1000, # 2118, Cell Signaling Technology, USA).

### *ALP analysis and staining*

For alkaline phosphatase (ALP) analysis, hBMSCs were collected using 0.25% trypsin and then frozen and thawed three times. The cell lysate supernatant was extracted by centrifugation at 12000 rpm for 10 min at 4 °C. PNPP was measured by adding 100 µL of DEA (50 mmol/L glycine and 1 mmol/L MgCl<sub>2</sub> at pH 10.5), 50 µL of PNPP solution (#N7653, Sigma, USA), and 50 µL of cell lysate supernatant to each well of a 96-well plate and incubating the plates for 15 min at 37 °C. After incubation, 400 µL of 1 N NaOH was added to each well to stop the reaction, and the absorbance was measured at 405 nm. The quantity of p-nitrophenol liberated from the substrate was determined by comparison to a standard curve. The total protein concentration was measured by a BCA assay. For this purpose, 200 µL of solution A (#23228, Pierce, USA), 4 µL of solution B (#1859078, Pierce, USA), and 20 µL of cell lysate supernatant were added to each well of a cell culture plate and incubated for 30 min at 37 °C; the absorbance was measured at 562 nm. ALP staining was performed using ALP staining reagent (Shanghai Hongqiao Le Xiang Institute of Biomedical, China) according to the manufacturer's instructions.

### *Tibial monocortical defect model*

The tibial monocortical defect model used in this study is a simplified stable fracture model, described previously [30, 31]. hBMSCs ( $5 \times 10^4$  cells per sample) isolated from patients with bone nonunion were collected at passage 3, resuspended in a mixture of medium and Matrigel (#356234, BD Bioscience, USA) and then transplanted to the osseous hole. After one month, tibiae were isolated, fixed overnight in 10% neutral buffered formalin, and kept in 70% ethanol until analysis, which was performed using a µCT35 system (SCANCO Medical) with a spatial resolution of 5 µm. Sagittal image sections of injured tibiae were used for 3D histomorphometric analysis.

### *Immunofluorescence assay*

Immunostaining was performed using a standard protocol. Sections were incubated overnight at 4 °C with the following primary antibodies: Chordin goat pAb (1:200, #sc-23557, Santa Cruz, USA) and phospho-Smad1/5/8 rabbit pAb (1:200, #4086, Cell Signaling Technology, USA). The primary antibodies were detected using a Cy3 or FITC-conjugated anti-goat or anti-rabbit IgG secondary antibody. After the final wash, the nuclei were counterstained with Hoechst 3342 (1:1000 #H3570, Life Technologies, USA) in PBS for 10 min before imaging. The stained sections were immediately observed by laser confocal microscopy (Cell Observer, ZEISS, Germany).

### *Statistical analysis*

All numerical data were expressed as the mean ± S.D. for the number of experiments performed. All statistical analyses were performed using SPSS software version 13.0. Statistical differences among groups were analysed by one-way analysis of variance with a post hoc test to determine group differences in the study parameters, and differences were considered statistically significant at \*,  $P < 0.05$  and \*\*,  $P < 0.01$ .

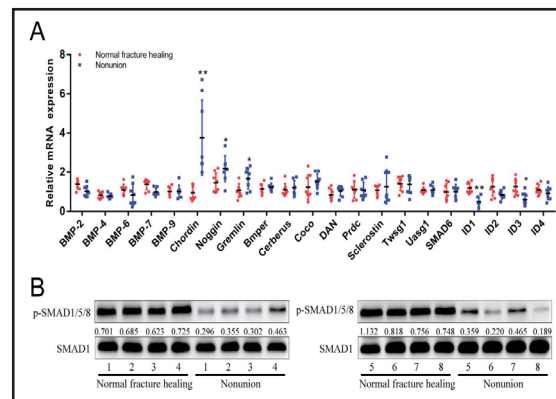
## Results

### *Expression of BMPs and BMP inhibitors in hBMSCs isolated from patients with bone nonunion and patients with normal fracture healing*

The expression of BMPs and BMP inhibitors in hBMSCs isolated from patients with bone nonunion has not yet been analysed. In the present study, hBMSCs were isolated from eight patients with bone nonunion and eight patients with normal fracture healing. The expression levels of Chordin, Noggin, and Gremlin were higher in hBMSCs isolated from patients with bone nonunion than in those isolated from patients with normal fracture healing, although

the expression of BMP-2 and BMP-4, as well as other BMPs and BMP inhibitors including BMP-6, BMP-9, Bmper, Cerberus, Coco, DAN, Prdc, Sclerostin, Twsg1 and Usag1, was not significantly different between the two groups (Fig. 1A). BMP-7 mRNA expression was decreased in patients with bone nonunion compared with patients with normal fracture healing. We next detected the mRNA expression of BMP target genes, including ID1, ID2, ID3 and ID4. The expression of ID1 and ID3 was down-regulated in hBMSCs from patients with bone nonunion, while the expression levels of ID2 and ID4 were not significantly different between the two groups of patients (Fig. 1G-I). In addition, Western blot results showed that the expression of p-SMAD1/5/8 was decreased in hBMSCs isolated from patients with bone nonunion. These results suggest that the BMP signalling pathway is inhibited in hBMSCs isolated from patients with bone nonunion.

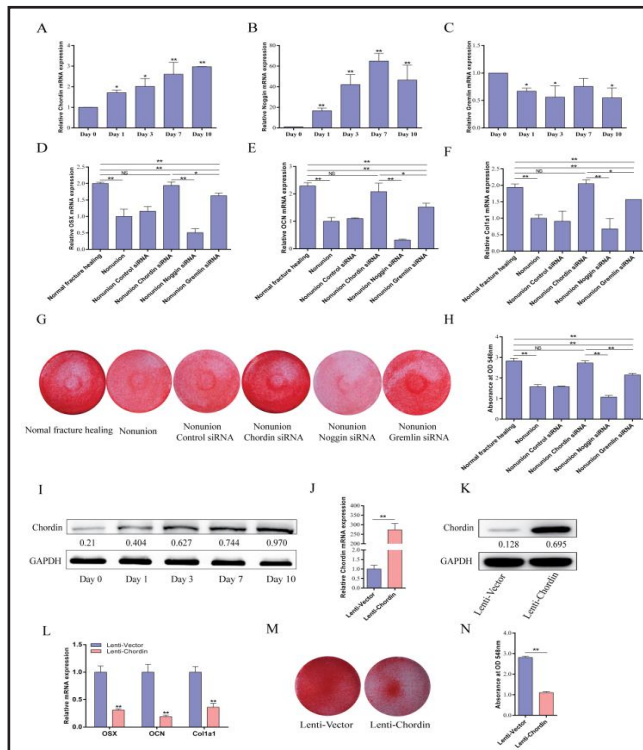
**Fig. 1.** mRNA expression of BMPs and BMP inhibitors in hBMSCs isolated from patients with bone nonunion and patients with normal fracture healing. (A) mRNA expression levels of BMPs and BMP inhibitors in hBMSCs isolated from patients with bone nonunion (N=8) and normal fracture healing (N=8) as measured by real-time PCR. (B) Western blot analysis of p-SMAD1/5/8 protein expression in hBMSCs isolated from patients with bone nonunion (N=8) and normal fracture healing (N=8). “\*\*\*” indicates P<0.01, “\*” indicates P<0.05.



*Chordin knockdown is an ideal target for enhancing the osteogenic differentiation of hBMSCs in patients with bone nonunion*

As we found that the BMP signalling pathway was inhibited in hBMSCs isolated from patients with bone nonunion, which showed higher expression of BMP inhibitors than cells from patients with normal healing fractures, we hypothesized that inhibiting the activity of BMP inhibitors could enhance the intrinsic activity of BMPs and promote the osteogenic differentiation of hBMSCs isolated from patients with bone nonunion. Chordin and Noggin mRNA expression increased during hBMSC osteogenesis (Fig. 2A and 2B). However, the expression of Gremlin decreased (Fig. 2C). To confirm the effect of Chordin, Noggin and Gremlin on hBMSC osteogenesis, we knocked down Chordin, Noggin and Gremlin expression using siRNAs in hBMSCs. Chordin knockdown promoted the expression of OSX, OCN, and Col1a1 more strongly than Gremlin knockdown in hBMSCs isolated from patients with bone nonunion (Fig. 2D-F). However, Noggin knockdown decreased the expression of OSX, OCN, and Col1a1 (Fig. 2D-F). After 21 days of osteogenic induction, Alizarin Red staining and quantitative detection demonstrated that hBMSCs isolated from patients with bone nonunion formed fewer mineralization nodules than hBMSCs isolated from patients with normal fracture healing (Fig. 2G and 2H). Chordin knockdown rescued the osteogenic ability of hBMSCs isolated from patients with bone nonunion (Fig. 2G and 2H). The expression of Chordin was further measured by Western blot, which confirmed that the induction of osteogenic differentiation was associated with increased Chordin expression (Fig. 2I). To further verify the role of Chordin in the osteogenic differentiation of hBMSCs, we overexpressed Chordin in hBMSCs using lentivirus (Fig. 2J and 2K). Chordin overexpression reduced the mRNA expression of OSX, OCN and Col1a1 in hBMSCs after 7 days of osteogenic introduction (Fig. 2L). Alizarin Red staining and quantitative detection indicated that Chordin overexpression reduced the osteogenic differentiation of hBMSCs (Fig. 2M and 2N). These results showed that Chordin is the most appropriate potential therapeutic target gene

**Fig. 2.** Chordin knockdown is an ideal target for enhancing the osteogenic differentiation of hBMSCs isolated from patients with bone nonunion. mRNA expression of Chordin (A), Noggin (B), and Gremlin (C) during the osteogenic differentiation of hBMSCs. The mRNA expression of OSX (D), OCN (E), and Col1a1 (F) in hBMSCs isolated from patients with bone normal bone fracture healing or with bone nonunion and transfected with NC siRNA, Chordin siRNA, Noggin siRNA or Gremlin siRNA after 7 days of osteogenic induction. (G) Alizarin Red S staining and (H) quantitative analysis of hBMSCs treated as indicated after 21 days of osteogenic induction. (I) Chordin protein expression during the osteogenic differentiation of hBMSCs as measured by Western blot. (J) Chordin mRNA expression in hBMSCs infected with Lenti-Vector or Lenti-Chordin after 3 days of culture. (K) Chordin protein expression in hBMSCs infected with Lenti-Vector or Lenti-Chordin after 3 days of culture. (L) The mRNA expression of OSX, OCN and Col1a1 in hBMSCs infected with Lenti-Vector or Lenti-Chordin after 7 days of osteogenic induction. (O) Alizarin Red S staining and (P) quantitative analysis of hBMSCs infected with Lenti-Vector or Lenti-Chordin after 21 days of osteogenic induction. The data presented are the result of three separate experiments. “\*” indicates  $P < 0.05$ , “\*\*” indicates  $P < 0.01$ , and “NS” means no significance.



among the tested BMP inhibitors for enhancing the osteogenic differentiation of hBMSCs isolated from patients with bone nonunion.

#### Cytotoxic effects of siRNA delivered by PSI and PSI/siRNA polyplexes to hBMSCs

Effective and nontoxic delivery is a key challenge and the most significant limitation to the therapeutic application of siRNA technology. Cytotoxicity is a major concern in the therapeutic application of a synthetic nucleic acid carrier. We next evaluated the cytotoxic effects of PSI on hBMSCs by performing an MTT assay. Similar to the spermine-treated group, the cell viability of hBMSCs remained unchanged even at a PSI polymer concentration of 100  $\mu\text{g}/\text{mL}$ . By contrast, the cell viability of PEI25kDa-treated hBMSCs dramatically dropped to 20% of the original value when the polymer concentration reached 15  $\mu\text{g}/\text{mL}$  (Fig. 3A). PSI/siRNA polyplexes at N/P ratios ranging from 5:1 to 100:1 also showed no negative effects on hBMSC viability (Fig. 3B); however, the cytotoxicity of PEI25kDa/siRNA polyplexes dramatically increased when N/P was greater than 20 (Fig. 3B).

Apoptosis was analysed after a 4-h incubation with hBMSCs, demonstrating that the PEI25kDa/siRNA polyplexes (N/P=20:1) induced a higher rate of apoptosis than the PSI/siRNA polyplexes (N/P=100:1) (Fig. 3C). Similarly, cell viability assays showed that the PEI25kDa/siRNA group exhibited significantly reduced cell viability compared with the PSI/siRNA and control groups (Fig. 3D). We subsequently investigated why fewer cells treated with PSI/siRNA underwent apoptosis. The highly positive charge of the polycation polymer compound may have interfered with the normal intracellular membrane potential; this phenomenon is also the main cause of cell apoptosis and reduced cell viability. The mitochondrial membrane potentials of hBMSCs incubated with PSI/siRNA and PEI25kDa/siRNA polyplexes for 4 h were determined by JC-1. hBMSCs incubated with PSI/siRNA showed

**Fig. 3.** Cytotoxic effects of siRNA delivered by PSI and PSI/siRNA polyplexes to hBMSCs. (A) Cytotoxicity of different vectors at concentrations ranging from 0.5  $\mu\text{g}/\text{mL}$  to 100  $\mu\text{g}/\text{mL}$ . (B) Cytotoxicity of different polyplexes with different N/P ratios. (C) Apoptosis of hBMSCs measured by Annexin V/PI staining. (D) Cell viability of hBMSCs measured using a LIVE/DEAD Viability/Cytotoxicity Assay Kit. Green: normal cells; red: dead cells. The scale is 100  $\mu\text{m}$ . (E) Mitochondrial membrane potentials of hBMSCs measured using JC-1 staining.

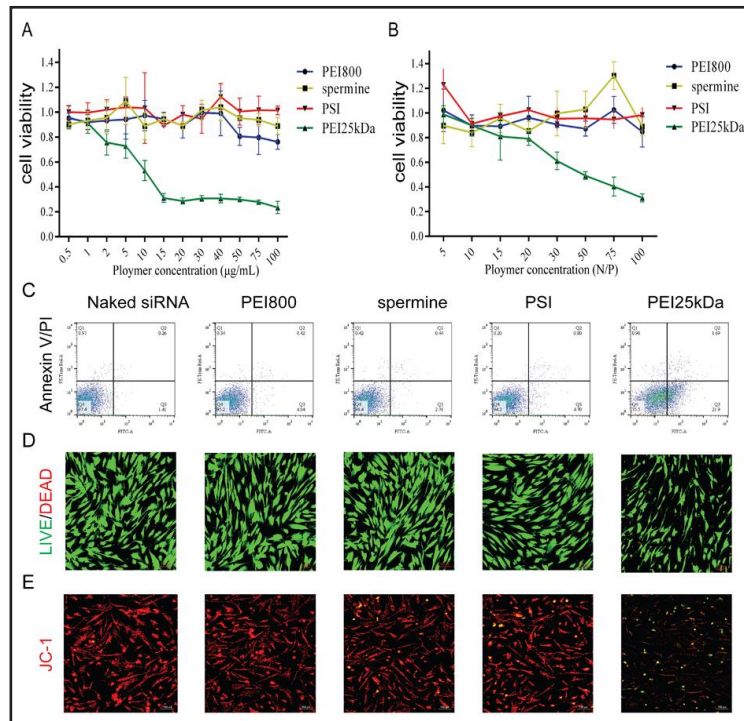
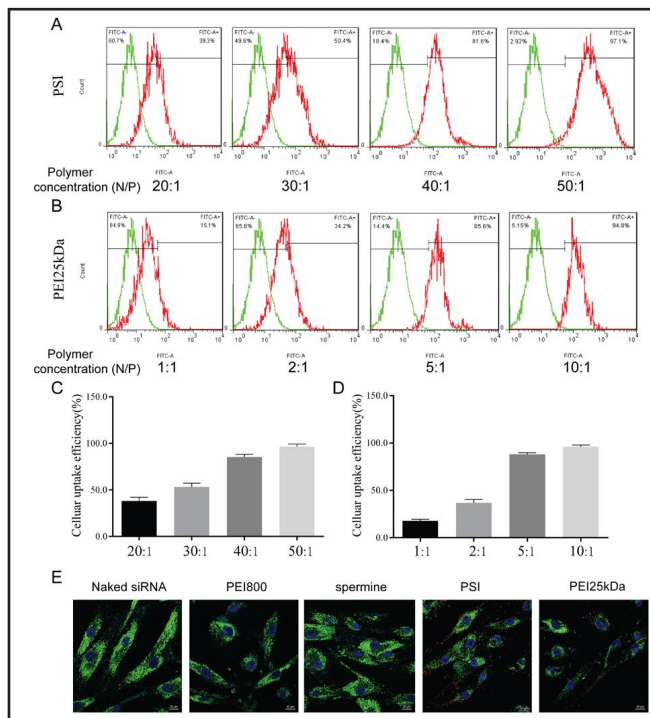


**Fig. 4.** Cellular uptake efficiency of PSI/siRNA polyplexes transfected into hBMSCs. (A) Representative flow cytometry images showing the cellular uptake efficiency of PSI/siRNA (A) and PEI25kDa/siRNA (B) polyplexes at different N/P ratios. Quantitative analysis of the cellular uptake efficiency of PSI/siRNA (C) and PEI25kDa/siRNA (D) polyplexes at different N/P ratios. (E) Cellular uptake of PSI/Cy3-siRNA and PEI25kDa/Cy3-siRNA polyplexes measured by confocal microscopy.



normal mitochondrial membrane potentials, while the mitochondrial membrane potentials of hBMSCs incubated with PEI25kDa/siRNA polyplexes were considerably reduced (Fig. 3E).

*Cellular uptake efficiency of PSI/siRNA polyplexes transfected into hBMSCs*

We compared the cellular uptake efficiency of PSI and PEI25kDa in delivering FITC-siRNA to hBMSCs. hBMSCs were transfected with PSI/FITC-siRNA polyplexes with various N/P ratios, and the uptake efficiencies were measured using flow cytometry. The transfection efficiencies in cells treated with PSI- and PEI25kDa-delivered FITC-siRNAs were 97.1% and 94.8% at the optimal N/P ratios of 50:1 and 10:1, respectively (Fig. 4A and 4B). These results indicated that the PSI/siRNA and PEI25kDa/siRNA polyplexes exhibited a high transfection



**Fig. 5.** Chordin knockdown efficiency of PSI/Chordin-siRNA polyplexes. Chordin expression measured by real-time PCR (A) and western blot (B) after transfection with PEI25kDa/Chordin-siRNA polyplexes and PSI/Chordin-siRNA polyplexes at different N/P ratios. Chordin expression measured by real-time PCR (C) and western blot (D) after transfection with PEI25kDa/Chordin-siRNA polyplexes (N/P ratio=20) and PSI/Chordin-siRNA polyplexes (N/P ratio=100) at days 0, 3, 7, 10, and 14. Chordin mRNA was normalized to GAPDH mRNA, data are represent as means  $\pm$  S.D. of three independent experiments, N=4. Chordin protein was normalized to GAPDH, Representative images of three independent experiments were shown. “\*” indicates P<0.05, “\*\*\*” indicates P<0.01, and “NS” means no significance.

efficiency, which increased as the N/P ratio increased (Fig. 4C and 4D). The cellular uptake of PSI/Cy3-siRNA (N/P=50:1) and PEI25kDa/Cy3-siRNA (N/P=10:1) polyplexes was also examined *via* confocal microscopy after 1 h of incubation with hBMSCs. We observed high cellular uptake of both PSI/Cy3-siRNA and PEI25kDa/Cy3-siRNA polyplexes (Fig. 4E).

#### Chordin knockdown efficiency of PSI/Chordin-siRNA polyplexes

To examine the knockdown efficiency of PSI/Chordin-siRNA, a Chordin-specific siRNA and a negative control siRNA were packaged into polyplexes with PSI and PEI25kDa at various N/P ratios and transfected into hBMSCs. Chordin mRNA expression was detected by real-time PCR and Western blot after 3 days of culture. The rates of Chordin silencing in the cells treated with PSI-delivered Chordin-specific siRNA (the PSI/Chordin-siRNA group) were 57.56%, 68.97%, and 81.89% at N/P ratios of 30:1, 40:1, and 50:1, respectively. By contrast, the rates of Chordin silencing in the cells treated with PEI25kDa-delivered Chordin-specific siRNA (the PEI25kDa/Chordin-siRNA group) were 57.14%, 74.71%, and 62.31% at N/P ratios of 5:1, 10:1, and 20:1, respectively (Fig. 5A–B). To determine the Chordin knockdown efficiency at different time points, we measured Chordin expression in hBMSCs at 3, 7, 10, and 14 days after transfection with PSI and PEI25kDa at their optimal N/P ratios of 50:1 and 10:1, respectively. We found that Chordin knockdown lasted for at least 10 days in both the PSI/Chordin-siRNA and PEI25kDa/Chordin-siRNA groups (Fig. 5C), and Western blot results confirmed this finding (Fig. 6D). In addition, Chordin mRNA expression was significantly lower in the PSI/Chordin-siRNA group than in the PEI25kDa/Chordin-siRNA group at 3 and 7 days after transfection (Fig. 5C–D). These results strongly suggest that PSI is superior to PEI25kDa in delivering Chordin-specific siRNA to hBMSCs and that the effect of Chordin knockdown can last for at least 10 days.

#### Osteogenic gene expression in hBMSCs transfected with PSI/Chordin-siRNA polyplexes

To evaluate the differentiation potential of hBMSCs, the gene expression of OSX, Col1a1 and OCN was measured by real-time PCR following transfection with Chordin-specific siRNA after 7 days of osteogenic differentiation. The mRNA expression levels of OSX, OCN, and Col1a1 markedly increased in the PSI/Chordin-siRNA and PEI25kDa/Chordin-siRNA groups

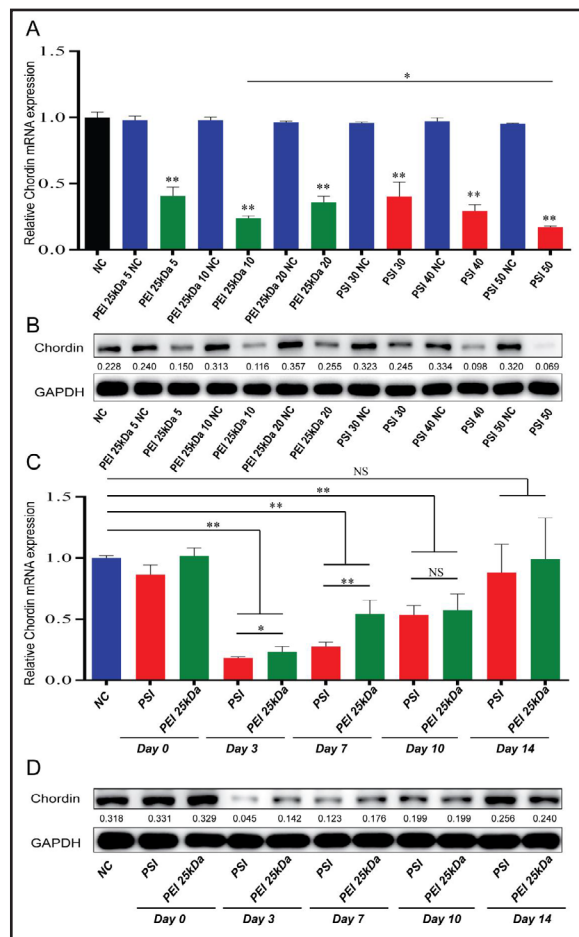


**Fig. 6.** Osteogenic gene expression in hBMSCs transfected with PSI/Chordin-siRNA polyplexes. The mRNA expression levels of OSX (A), OCN (B), and Col1a1 (C) in hBMSCs transfected with different polyplexes after 7 days osteogenic induction using BMP-2 were measured by real-time PCR. The expression levels of Runx2 and p-SMAD1/5/8 complexes in hBMSCs transfected with different polyplexes after 7 days osteogenic induction using BMP-2(D),BMP-4(E), BMP-7(F), BMP-6(G), BMP-9(H) were measured by Western blot. RUNX2 and p-SMAD1/5/8 protein levels were normalized to GAPDH and SMAD1, respectively. Representative images of three repeated experiments were shown. "\*" indicates  $P < 0.05$ , "\*\*" indicates  $P < 0.01$ , and "NS" means no significance.

compared with the spermine/Chordin-siRNA, PEI800/Chordin-siRNA, and NC (naked siRNA) groups; moreover, the expression levels of these genes were significantly higher in the PSI/Chordin-siRNA group than in the PEI25kDa/Chordin-siRNA group (Fig. 6A–6C). Western blot results showed that the expression levels of p-SMAD1/5/8 and Runx2 increased in the PSI/Chordin-siRNA and PEI25kDa/Chordin-siRNA groups compared with those in the spermine/Chordin-siRNA, PEI800/Chordin-siRNA, and NC (naked siRNA) groups after incubation in OM, indicating that the BMP signalling pathway was activated when the expression of the BMP-2 inhibitor Chordin was knocked down (Fig. 6D). Moreover, the expression levels of Runx2 and p-SMAD1/5/8 were higher in the PSI/Chordin-siRNA group than in the PEI25kDa/Chordin-siRNA group. Because Chordin primarily binds to BMP-2, BMP-4 and BMP-7, but not BMP-6 and BMP-9, we detected the expression levels of Runx2 and p-SMAD1/5/8 in hBMSCs transfected with Chordin-siRNA after osteogenic induction using BMP-4, BMP-7, BMP-6 and BMP-9 at 100 ng/mL. When BMP-4 and BMP-7 were used as osteogenic inducers, the expression levels of Runx2 and p-SMAD1/5/8 increased in the PSI/Chordin-siRNA and PEI25kDa/Chordin-siRNA groups compared with the NC group (Fig. 6E and 6F). However, when BMP-6 and BMP-9 were used as osteogenic inducers, the expression levels of Runx2 and p-SMAD1/5/8 were unchanged in the PSI/Chordin-siRNA and PEI25kDa/Chordin-siRNA groups compared with the NC group (Fig. 6G and 6H).

*Chordin knockdown rescued the osteogenic capacity of hBMSCs isolated from patients with bone nonunion*

ALP activity was significantly enhanced and ALP staining markedly increased in hBMSCs at 7 days (Fig. 7A and 7C) and 14 days (Fig. 7B and 7D) post-transfection with Chordin-specific siRNA via PSI and PEI25kDa polyplexes compared with the spermine/Chordin-siRNA, PEI800/Chordin-siRNA and NC (naked siRNA) groups. The ALP activity in the PSI/Chordin-siRNA group was 1.29 and 1.41 times higher than that of the PEI25kDa/Chordin-siRNA group at 7 and 14 days, respectively. Inhibition of Chordin expression improved Alizarin red staining, and the PSI/Chordin-siRNA and PEI25kDa/Chordin-siRNA groups showed deeper staining than the spermine/Chordin-siRNA, PEI800/Chordin-siRNA, and NC (naked

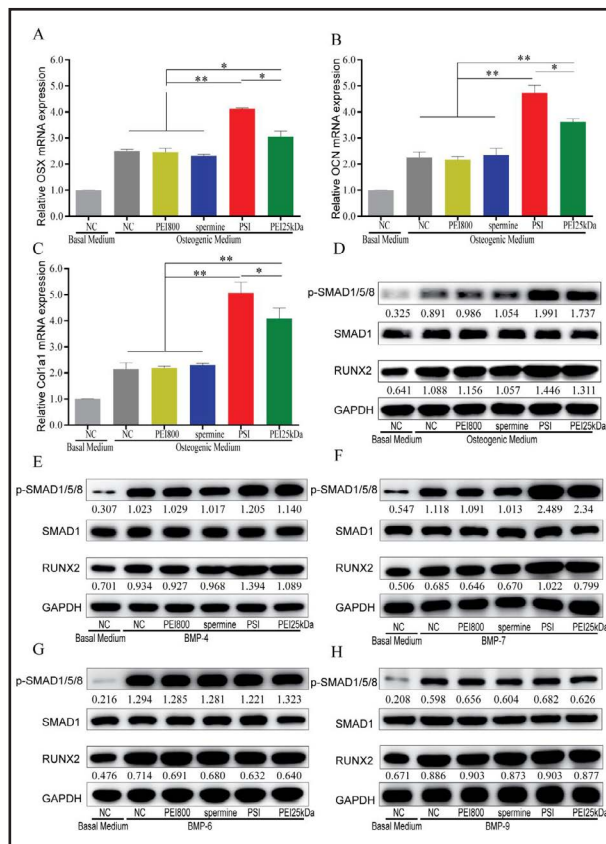
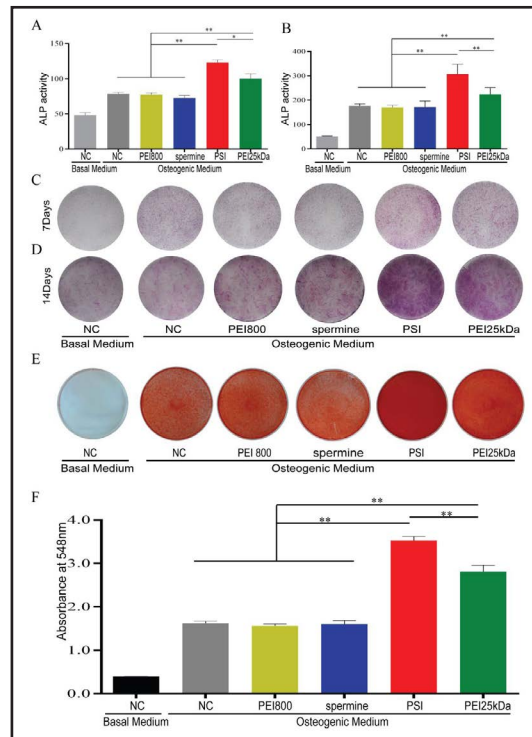


**Fig. 7.** Chordin knockdown rescued the osteogenic capacity of hBMSCs isolated from patients with bone nonunion. ALP activity of hBMSCs transfected with different polyplexes were measured after 7 days (A) and 14 days (B) osteogenic introduction. ALP staining of hBMSCs transfected with different polyplexes were measured after 7 days (C) and 14 days (D) osteogenic introduction. (E) Alizarin Red S staining of hBMSCs transfected with different polyplexes were measured after 21 days of osteogenic induction. (F) Quantitative analysis of Alizarin Red S staining. Data are presented as means  $\pm$  S.D. of three independent experiments, N=5. “\*” indicates  $P < 0.05$ , “\*\*” indicates  $P < 0.01$ .



siRNA) groups (Fig. 7E). In addition, the PSI/Chordin-siRNA group exhibited significantly deeper staining than the PEI25kDa/Chordin-siRNA group. Alizarin red staining was also quantified by spectrophotometry at 548 nm, which showed that knockdown of Chordin expression significantly improved calcium deposition in mineralized nodules, and the calcium deposition in the matrix in the PSI/Chordin-siRNA group was nearly 1.23 times higher than that observed in the PEI25kDa/Chordin-siRNA group (Fig. 7F). These analyses provided quantitative and qualitative evidence that inhibition of Chordin expression rescued the osteogenic capacity of hBMSCs isolated from patients with bone nonunion and that PSI/Chordin-siRNA exerted a stronger effect on hBMSCs than PEI25kDa/Chordin-siRNA.

*Chordin knockdown promoted the bone regeneration of hBMSCs isolated from patients with bone nonunion in vivo*

To investigate the function of Chordin inhibition *in vivo*, we determined the osteogenic activity of hBMSCs transfected with Chordin-specific siRNA by using a tibial monocortical defect model. hBMSCs isolated from patients with bone nonunion were transfected with Chordin siRNA using PSI, PEI25kDa, spermine, and PEI800 and were subsequently mixed with Matrigel and transplanted into the osseous hole.  $\mu$ CT was used to quantify the newly formed bone in the defect one month after hBMSC transplantation. Lateral views of the 3D reconstruction of the injured tibia showed more mineralized tissue in the PSI/Chordin-siRNA group than in the PEI25kDa/Chordin-siRNA group, and the areas of mineralized tissue were smallest in the PEI800/Chordin-siRNA, spermine/Chordin-siRNA and NC groups (Fig. 8A). Compared with the PEI25kDa/Chordin-siRNA group, bone mineral density (BMD), bone volume density (BV/TV), trabecular number (Tb.N), and trabecular thickness (Tb.Th) increased in the PSI/Chordin-siRNA group by approximately 1.33, 1.18, 1.18 and 1.16 times, respectively (Fig. 8B-E). Conversely, trabecular separation (Tb.Sp) was reduced by 41% in the PSI/Chordin-siRNA group compared with the PEI25kDa/Chordin-siRNA group (Fig. 8F). New bone formation was also revealed by H&E staining, and the new bone formation area was larger in the PSI/Chordin-siRNA group than in the PEI25kDa/Chordin-siRNA group, while the new bone formation areas were quite small in the PEI800/Chordin-siRNA, spermine/Chordin-siRNA and NC group (Fig. 8G). Because Chordin is a secreted protein, we detected Chordin and p-Smad1/5/8 in the fibrous tissue around newly formed bone. Chordin expression was higher in the PEI800/Chordin-siRNA, spermine/Chordin-siRNA and NC groups than in the PSI/Chordin-siRNA than PEI25kDa/Chordin-siRNA groups (Fig. 8H). Very little Chordin expression was detected in the fibrous tissue around newly formed bone in the PSI/Chordin-siRNA group. In addition, p-SMAD1/5/8 expression was higher in

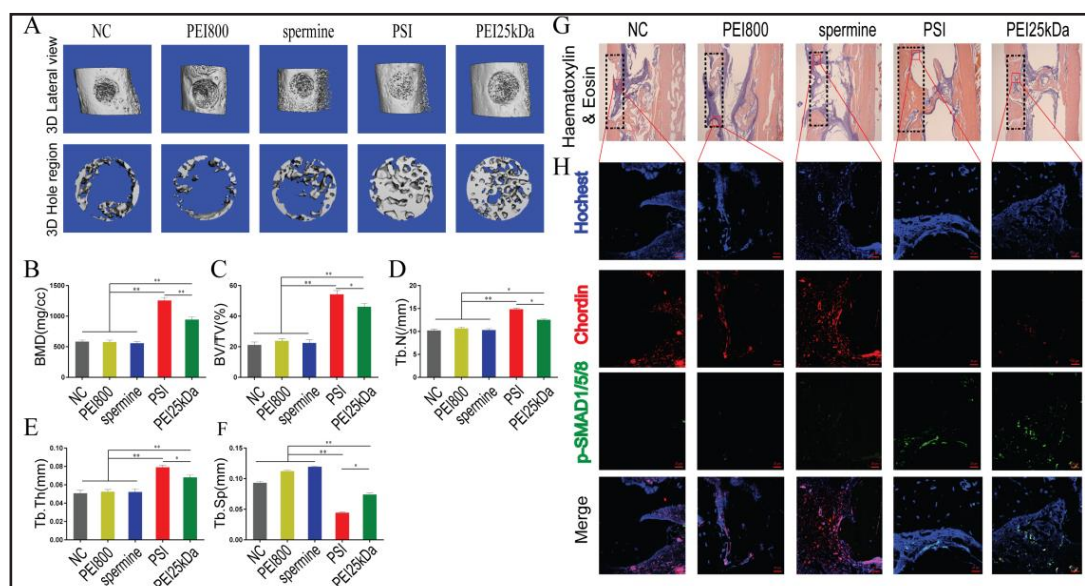


**Fig. 8.** Chordin knockdown promoted the bone regeneration of hBMSCs isolated from patients with bone nonunion *in vivo* (A) Lateral views of 3D reconstruction of injured tibiae (top panel) and mineralized bone formed in hole region (lower panel) by  $\mu$ CT. Representative images from of each group, N=5. (B-F) 3D structural parameters- BMD, BV/TV, Tb.N., Tb.Th and Tb.Sp-of mineralized bone formed in hole region by  $\mu$ CT, N=5. (F) Representative images of H&E staining (top panel) showed new bone formation in injured tibiae (black frame). (H) Immunofluorescent assay of Chordin and p-SMAD1/5/8 expression in fibrous tissue around new bone. The scale is 20  $\mu$ m, Blue: cell nucleus, Red: Chordin, Green: p-SMAD1/5/8. “\*” indicates  $P < 0.05$ , “\*\*\*” indicates  $P < 0.01$ .

the PSI/Chordin-siRNA and PEI25kDa/Chordin-siRNA groups than in the PEI800/Chordin-siRNA, spermine/Chordin-siRNA and NC groups (Fig. 8H). These results indicate that Chordin knockdown promoted the bone regeneration ability of hBMSCs isolated from patients with bone nonunion *in vivo*. PSI/Chordin-siRNA polyplexes were more able to promote the bone regeneration ability of hBMSCs than PEI25kDa/Chordin-siRNA polyplexes.

## Discussion

Bone nonunion is a challenging problem that may occur following certain bone fractures. However, there has been little investigation of the molecular basis of bone nonunion [2]. BMPs and BMP inhibitors play a significant role in osteogenesis. Niikura et al. compared the global gene expression levels of osteogenic BMPs and their inhibitors in rat fracture and atrophic bone nonunion tissues and proposed that the imbalance between BMPs and BMP inhibitors may be a potential cause of the development of bone nonunion [2]. Other teams have investigated the same question; however, the results have been inconsistent [32-34]. Although these studies all found that there was an imbalance between BMPs and BMP inhibitors in bone nonunions compared with fractures that heal normally, it remains unclear whether bone nonunion is caused by suboptimal expression of BMPs, by increased expression of BMP inhibitors, or possibly by both of these factors. These discrepancies may be explained by differences in the timing of the bone nonunion analysis, species used, location of the bone nonunion and the type of bone nonunion [14]. Currently, no studies have reported the difference in the expression of BMPs and BMP inhibitors in hBMSCs isolated from patients with normal fracture healing and those with bone nonunion. The results of our study indicate that the mRNA expression pattern of endogenous BMPs and BMP inhibitors in hBMSCs isolated from patients with bone nonunion was different from that of hBMSCs isolated from patients with normal fracture healing. Specifically, our results show that the expression of BMP-7 was decreased and that of Chordin, Noggin and Gremlin was increased in hBMSCs

isolated from patients with bone nonunion. In addition, the osteogenic differentiation ability of hBMSCs isolated from patients with bone nonunion was lower than that of hBMSCs isolated from patients with normal fracture healing. Meanwhile, the expression of the BMP target genes ID1, ID3 and p-SMAD1/5/8 decreased in hBMSCs isolated from patients with bone nonunion. By knocking down the expression of Chordin, Noggin and Gremlin in hBMSCs with specific siRNAs, we found that Chordin knockdown most strongly increased the osteogenic differentiation of hBMSCs. Therefore, we hypothesized that Chordin was an ideal target for rescuing the osteogenic differentiation of hBMSCs isolated from patients with bone nonunion. Our studies revealed that hBMSCs isolated from patients with bone nonunion exhibited decreased BMP expression and increased BMP inhibitor expression. BMP-2 and BMP-7 play important roles in bone regeneration and are both FDA-approved for clinical use in fracture healing, long bone nonunion, periodontal and dental applications and spinal fusions [16]. However, concerns remain regarding the safety and cost-effectiveness of their clinical application. For example, adverse effects such as osteolysis, infection, arachnoiditis, increased neurological deficits and retrograde ejaculation have been reported after the use of BMP-2 [35]. A sufficient number of studies have shown that BMP inhibitors play a major role in bone regeneration. So far, no studies have attempted to block one or more BMP inhibitors to accelerate fracture healing in humans. Some studies have indicated that a high dose of BMPs could increase the expression of BMP inhibitors, limiting the functional therapeutic application of BMPs [14]. Therefore, we hypothesized that Chordin knockdown could maximize BMP activity and eliminate the need for expensive, high-dose exogenous BMP treatment.

siRNA transfection is a powerful tool for identifying the mechanism of a given disease and provides a promising therapeutic method for gene-related diseases. A feasible nucleic acid vector with biocompatibility, multifunctionality, stimulus responsiveness, high loading capacity and high transfection efficiency is needed to accomplish the inter- and intracellular trafficking required for siRNA delivery. Recently, we developed an siRNA vector known as PSI by condensing spermine and bisformaldehyde imidazole through a pH-responsive linkage, a bis-imine bond conjugated with the imidazole. In our previous study, we showed that PSI could be degraded into imidazole-biscarboxylic acid, a safe metabolite of cefpimizole sodium and spermine. In our study, we found that spermine had no toxic effects on hBMSCs. We also found that PSI was non-toxic to hBMSCs using various methods, while PEI25kDa exhibited some cytotoxicity. PEI is reportedly an apoptotic agent, and some studies have also shown that the apoptosis of cells mediated by PEI-based vectors depends on mitochondrial membrane damage, as the mitochondrial membrane potential decreases after PEI transfection [23]. We measured the mitochondrial membrane potential by JC-1 staining after transfection with PEI25kDa and PSI and found that cells transfected with PSI had reduced mitochondrial membrane damage compared with cells transfected with PEI25kDa. The degradation of PSI may account for the lower mitochondrial membrane damage. We next detected the cellular uptake of PSI/siRNA polyplexes and PEI25kDa/siRNA polyplexes using flow cytometry and laser confocal microscopy. Both groups had high cellular uptake efficiency. We also measured the Chordin knockdown efficiency using PSI and PEI25kDa polyplexes at different N/P ratios. Transfection with PSI polyplexes resulted in a higher knockdown efficiency than transfection with PEI25kDa polyplexes at optimal N/P ratios. Subsequently, we detected the Chordin knockdown efficiency at 3 days, 7 days, 10 days and 14 days after transfection with PSI and PEI25kDa polyplexes at optimal N/P ratios. PSI polyplexes exhibited a higher knockdown efficiency than PEI25kDa polyplexes at 3 days and 7 days. This may be because PSI can degrade rapidly to release siRNA into the cytoplasm, resulting in a stronger effect on gene knockdown and higher cell viability. In addition, hBMSCs in the PSI group had stronger osteogenic differentiation ability than those in the PEI25kDa group. We used the tibial monocortical defect model to investigate the function of Chordin inhibition *in vivo* and found that Chordin knockdown obviously promoted the bone regeneration ability of hBMSCs. This is the first report that Chordin knockdown could promote the osteogenic differentiation of hBMSCs isolated from patients with bone nonunion.

## Conclusion

We found that Chordin knockdown increased the osteogenic differentiation and rescued the osteogenic capacity of hBMSCs isolated from patients with bone nonunion. PSI polyplexes exhibited a higher Chordin knockdown efficiency than PEI25kDa polyplexes in hBMSCs. We found that Chordin knockdown enhanced the BMP-2 pathway by increasing the expression of the p-SMAD1/5/8 complex and promoted osteogenesis and bone regeneration of hBMSCs isolated from patients with bone nonunion *in vitro* and *in vivo*. Thus, Chordin is a potential target for improving osteogenesis and bone nonunion therapy, and the packaging of Chordin siRNA with PSI is a promising method for clinical application owing to its high siRNA delivery efficiency and negligible cytotoxicity.

## Acknowledgements

This work was supported by grants from National Natural Science Foundation of China (No.81772347, 81572123), Science and Technology Commission of Shanghai Municipality (No.15411951100, 16430723500), Shanghai Municipal Education Commission-Gaofeng Clinical Medicine Grant Support (No.20161314) and Shanghai Shen Kang hospital development center (No. 16CR2036B), China Postdoctoral Science Foundation (No.2017M621501).

## Disclosure Statement

The authors report no conflicts of interest in this work.

## References

- 1 Conway JD, Shabtai L, Bauernschub A, Specht SC: Bmp-7 versus bmp-2 for the treatment of long bone nonunion. *Orthopedics* 2014;37:e1049-1057.
- 2 Niikura T, Hak DJ, Reddi AH: Global gene profiling reveals a downregulation of bmp gene expression in experimental atrophic nonunions compared to standard healing fractures. *J Orthop Res* 2006;24:1463-1471.
- 3 Zhao X, Qu Z, Tickner J, Xu J, Dai K, Zhang X: The role of satb2 in skeletogenesis and human disease. *Cytokine Growth Factor Rev* 2014;25:35-44.
- 4 Chen C, Uludag H, Wang Z, Jiang H: Noggin suppression decreases bmp-2-induced osteogenesis of human bone marrow-derived mesenchymal stem cells *in vitro*. *J Cell Biochem* 2012;113:3672-3680.
- 5 Zhang C, Li L, Feng K, Fan D, Xue W, Lu J: 'Repair' treg cells in tissue injury. *Cell Physiol Biochem* 2017;43:2155-2169.
- 6 Zhou W, Yu L, Fan J, Wan B, Jiang T, Yin J, Huang Y, Li Q, Yin G, Hu Z: Endogenous parathyroid hormone promotes fracture healing by increasing expression of bmp2 through camp/pka/creb pathway in mice. *Cell Physiol Biochem* 2017;42:551-563.
- 7 Huang J, Peng J, Cao G, Lu S, Liu L, Li Z, Zhou M, Feng M, Shen H: Hypoxia-induced microRNA-429 promotes differentiation of mc3t3-e1 osteoblastic cells by mediating zfp2 expression. *Cell Physiol Biochem* 2016;39:1177-1186.
- 8 Gao Y, Zhang Y, Lu Y, Wang Y, Kou X, Lou Y, Kang Y: Tob1 deficiency enhances the effect of bone marrow-derived mesenchymal stem cells on tendon-bone healing in a rat rotator cuff repair model. *Cell Physiol Biochem* 2016;38:319-329.
- 9 de la Croix Ndong J, Makowski AJ, Uppuganti S, Vignaux G, Ono K, Perrien DS, Joubert S, Baglio SR, Granchi D, Stevenson DA, Rios JJ, Nyman JS, Elefteriou F: Asfotase-alpha improves bone growth, mineralization and strength in mouse models of neurofibromatosis type-1. *Nat Med* 2014;20:904-910.
- 10 Yu B, Zhao X, Yang C, Crane J, Xian L, Lu W, Wan M, Cao X: Parathyroid hormone induces differentiation of mesenchymal stromal/stem cells by enhancing bone morphogenetic protein signaling. *J Bone Miner Res* 2012;27:2001-2014.
- 11 Wang X, Guo B, Li Q, Peng J, Yang Z, Wang A, Li D, Hou Z, Lv K, Kan G, Cao H, Wu H, Song J, Pan X, Sun Q, Ling S, Li Y, Zhu M, Zhang P, Peng S, Xie X, Tang T, Hong A, Bian Z, Bai Y, Lu A, Li Y, He F, Zhang G, Li Y: Mir-214 targets atf4 to inhibit bone formation. *Nat Med* 2013;19:93-100.

- 12 Chen G, Deng C, Li YP: Tgf-beta and bmp signaling in osteoblast differentiation and bone formation. *Int J Biol Sci* 2012;8:272-288.
- 13 Zou L, Zhang G, Liu L, Chen C, Cao X, Cai J: A microrna-124 polymorphism is associated with fracture healing via modulating bmp6 expression. *Cell Physiol Biochem* 2017;41:2161-2170.
- 14 Kloen P, Lauzier D, Hamdy RC: Co-expression of bmps and bmp-inhibitors in human fractures and non-unions. *Bone* 2012;51:59-68.
- 15 Axelrad TW, Einhorn TA: Bone morphogenetic proteins in orthopaedic surgery. *Cytokine Growth Factor Rev* 2009;20:481-488.
- 16 Balmayor ER, Geiger JP, Aneja MK, Berezhanskyy T, Utzinger M, Mykhaylyk O, Rudolph C, Plank C: Chemically modified rna induces osteogenesis of stem cells and human tissue explants as well as accelerates bone healing in rats. *Biomaterials* 2016;87:131-146.
- 17 Hinsenkamp M, Collard JF: Growth factors in orthopaedic surgery: Demineralized bone matrix versus recombinant bone morphogenetic proteins. *Int Orthop* 2015;39:137-147.
- 18 Meinhardt H: Dorsoventral patterning by the chordin-bmp pathway: A unified model from a pattern-formation perspective for drosophila, vertebrates, sea urchins and nematostella. *Dev Biol* 2015;405:137-148.
- 19 Walsh DW, Godson C, Brazil DP, Martin F: Extracellular bmp-antagonist regulation in development and disease: Tied up in knots. *Trends Cell Biol* 2010;20:244-256.
- 20 Tsiologiannis E, Polyzois I, Oak Tang Q, Pavlou G, Tsiroidis E, Heliotis M, Tsiroidis E: Targeting bone morphogenetic protein antagonists: *In vitro* and *in vivo* evidence of their role in bone metabolism. *Expert Opin Ther Targets* 2009;13:123-137.
- 21 Sanchez-Duffhues G, Hiepen C, Knaus P, Ten Dijke P: Bone morphogenetic protein signaling in bone homeostasis. *Bone* 2015;80:43-59.
- 22 Duan S, Yuan W, Wu F, Jin T: Polyspermine imidazole-4, 5-imine, a chemically dynamic and biologically responsive carrier system for intracellular delivery of sirna. *Angew Chem Int Ed Engl* 2012;51:7938-7941.
- 23 Xiang S, Su J, Tong H, Yang F, Tong W, Yuan W, Wu F, Wang C, Jin T, Dai K, Zhang X: Biscarbamate cross-linked low molecular weight pei for delivering il-1 receptor antagonist gene to synoviocytes for arthritis therapy. *Biomaterials* 2012;33:6520-6532.
- 24 Boussif O, Lezoualc'h F, Zanta MA, Mergny MD, Scherman D, Demeneix B, Behr JP: A versatile vector for gene and oligonucleotide transfer into cells in culture and *in vivo*: Polyethylenimine. *Proc Natl Acad Sci U S A* 1995;92:7297-7301.
- 25 Bonnet ME, Erbacher P, Bolcato-Bellemin AL: Systemic delivery of DNA or sirna mediated by linear polyethylenimine (l-pei) does not induce an inflammatory response. *Pharm Res* 2008;25:2972-2982.
- 26 Kapilov-Buchman Y, Lellouche E, Michaeli S, Lellouche JP: Unique surface modification of silica nanoparticles with polyethylenimine (pei) for sirna delivery using cerium cation coordination chemistry. *Bioconjug Chem* 2015;26:880-889.
- 27 Duan SY, Ge XM, Lu N, Wu F, Yuan W, Jin T: Synthetic polyspermine imidazole-4, 5-amide as an efficient and cytotoxicity-free gene delivery system. *Int J Nanomedicine* 2012;7:3813-3822.
- 28 Whitehead KA, Langer R, Anderson DG: Knocking down barriers: Advances in sirna delivery. *Nat Rev Drug Discov* 2009;8:129-138.
- 29 Abdallah BM, Ditzel N, Kassem M: Assessment of bone formation capacity using *in vivo* transplantation assays: Procedure and tissue analysis. *Methods Mol Biol* 2008;455:89-100.
- 30 Hu K, Olsen BR: Osteoblast-derived vegf regulates osteoblast differentiation and bone formation during bone repair. *J Clin Invest* 2016;126:509-526.
- 31 Yamamoto K, Kishida T, Sato Y, Nishioka K, Ejima A, Fujiwara H, Kubo T, Yamamoto T, Kanamura N, Mazda O: Direct conversion of human fibroblasts into functional osteoblasts by defined factors. *Proc Natl Acad Sci U S A* 2015;112:6152-6157.
- 32 Kwong FNK, Hoyland JA, Freemont AJ, Evans CH: Altered relative expression of bmps and bmp inhibitors in cartilaginous areas of human fractures progressing towards nonunion. *J Orthop Res* 2009;27:752-757.
- 33 Dean DB, Watson JT, Jin W, Peters C, Enders JT, Chen A, Moed BR, Zhang Z: Distinct functionalities of bone morphogenetic protein antagonists during fracture healing in mice. *J Anat* 2010;216:625-630.
- 34 Yu YY, Lieu S, Lu C, Miclau T, Marcucio RS, Colnot C: Immunolocalization of bmps, bmp antagonists, receptors, and effectors during fracture repair. *Bone* 2010;46:841-851.
- 35 Chrastil J, Low JB, Whang PG, Patel AA: Complications associated with the use of the recombinant human bone morphogenetic proteins for posterior interbody fusions of the lumbar spine. *Spine* 2013;38:E1020-E1027.